Proceedings World Geothermal Congress 2015
Melbourne, Australia, 19-25 April 2015

THM Modelling of Hydrothermal Circulation in Deep Geothermal Reservoirs

Vincent Magnenet (1), Christophe Fond (1), Jean Schmittbuhl (2), Clément Baujard (3), and Albert Genter (3)

(1) ICUBE, UMR CNRS 7357, 72, Route du Rhin CS 315, F-67411 ILLKIRCH Cedex, France
(2) EOST, CNRS/UdS, 5 rue René Descartes, F-67084 STRASBOURG Cedex, France
(3) ES-Géothermie, 26 Boulevard du Président Wilson, F-67000Strasbourg, France

Vincent.Magnenet@unistra.fr

Keywords: Soultz-sous-Forêts project, Hydrothermal convection, thermo-poro-elasticity, granite reservoir

ABSTRACT

Numerous models have been developed for describing deep geothermal reservoirs. Using the open source finite element software ASTER developed by EDF R&D, we carried out 2D simulations of the hydrothermal circulation in the deep geothermal reservoir of Soultz-sous-Forêts (France). The model is based on the effective description of Thermo-Hydro-Mechanical (THM) coupling at large scale. The reservoir is described at large scale (about 10 km in width and 5 km in height) and it is assumed that the medium is homogenous, porous, and saturated with single-phase fluid (considering homogenized effective porous and/or fractured layers, neglecting the complexity of the fracture networks). We introduced not only poro-elastic behavior of the rock matrix but also the sensitivity of the fluid density, viscosity, and heat capacity to temperature and pressure. The behavior of solid rock grains is assumed to be isotropic thermo-elastic and linear. Hydraulic and thermal phenomena are governed by Darcy and Fourier laws respectively, and most rock properties (like the specific heat at constant stress C_s^σ (T), or the thermal conductivity λ(T,φ)) are assumed to depend on the temperature T and/or porosity φ. The radioactivity of the rocks is taken into account through a heat source term appearing in the balance equation of enthalpy. To characterize as precisely as possible the convective movement of water and the associated heat flow, water properties (specific mass ρ_w (T,p_w), specific enthalpy), h_w^m(T,p_w) dynamic viscosity μ_w (T), thermal dilation α_w (T), and specific heat C_w^p (T)) are assumed to depend on pressure and/or temperature. The entire set of material properties is extracted from references dealing with investigations done at Soultz-sous-Forêts when existing. We aim at showing that stable solutions with large scale hydrothermal convective cells compatible with field observations do exist without accounting for local major faults and discuss the implications for the role of major faults on the regional fluid circulations. We also address the possible stress perturbations related to temperature fluctuations at large scales and their implications on induced seismicity.

1. INTRODUCTION

Several models have been developed in the literature to reproduce field measurements or to predict the value of physical properties in deep geothermal reservoirs. The most simplified approaches are one-dimensional. They couple hydraulic with thermics as in Pasquale et al. (2011), but more complex geometries have been considered in two dimensions as in Guillou-Frottier et al. (2013); Kohl et al. (2000); Cerminara and Fasano (2012) or in three dimensions, Bächler et al. (2003); Kohl and Mégel (2007). Most of these models aim at reproducing or predicting the temperature profile measured in wells and/or hydraulic data obtained during injection and production phases (water flow, water pressure and temperature vs. time). Some numerical models have also been developed to account for mechanical, thermal and hydraulic couplings at the same time, with a simplified geometry of the fault network, see e.g. Kohl et al. (1995) or Gelet et al. (2012). In addition, other thermodynamical aspects have been addressed like chemical coupling in Bächler and Kohl (2005).

The present work is in line with these previous approaches and can be viewed as another thermo-hydro-mechanical (THM) model of the Soultz-sous-Forêts geothermal reservoir. We consider the latter at large scale (about 10km in width and 5km in height). Our specificity is to assume that media are homogenized — i.e. at a scale above the representative elementary volume (REV) — as porous materials saturated with a single-phase fluid but including all major THM couplings. Our work is limited to a two-dimensional modeling, as in the recent contribution from Guillou-Frottier et al. (2013). The main geological structures retained here are (i) the main sedimentary beddings of the Rhine Graben and (ii) major petrographic transitions in the granite, which are supposed to be horizontal. No fault is included in the model at this stage. Despite these strong geometrical assumptions, we aim at accounting for the various rheologies of rocks and water, which constitute the main contribution of the present work compared to the above mentioned studies.

The interest of obtaining a numerical and coupled model of a given geothermal reservoir is fourfold. At first, it allows the physical integration of laboratory measurements (rock physics), such as well logging, well head parameters, geological description, and geophysics field measurements. It shows how data are precious input parameters of the model, and gives them a utility of great importance. Secondly, it provides a direct model based for geophysical inversion of field measurements: fluid flow, fluid pressure, temperature profile, seismicity monitoring, deformation of the ground surface (INSAR/GPS) related to reservoir modification, gravity or electromagnetic geophysical measurements. Thirdly, another advantage of simulating the reservoir behavior is the possibility to analyze the sensitivities of parameters involved in the hydrothermal circulation (or in other physical processes). This analysis can lead to the identification of material properties having the greatest influence on the model outputs, thus providing useful information for the planning of new experimental investigations. Finally, the model can also be used as a decision tool for drilling and emplacement planning, stimulation and exploitation.

2. GOVERNING EQUATIONS

The constitutive equations used in this work are those of fluid saturated porous media with THM couplings. Three forms of energy are considered: mechanical, thermal and hydraulic energies. Small perturbation assumption is made. In doing so, no confusion between Eulerian and Lagrangian operators is then possible. The balance equations driving the evolution of extensive quantities associated with all forms of energies write:

$$\nabla \cdot \boldsymbol{\sigma} + \rho \boldsymbol{F}^m = 0 \quad \textit{(momentum balance)} \tag{1}$$

$$\frac{\partial m_w}{\partial t} + \nabla \cdot \boldsymbol{M}_w = 0 \quad \textit{(mass balance)} \tag{2}$$

$$\boldsymbol{M}_w \cdot \boldsymbol{F}^m + \theta = h_w^m \frac{\partial m_w}{\partial t} + \dot{Q} + \nabla \cdot (h_w^m \boldsymbol{M}_w) + \nabla \cdot \boldsymbol{q} \quad \textit{(energy balance)} \tag{3}$$

where $\boldsymbol{\sigma}$ [Pa] is the Cauchy stress tensor, ρ [kg.m^{-3}] the total homogenized specific mass, and $\boldsymbol{F}^m$ the mass force density (gravity in the present paper). In this work, ρ is decomposed into two contributions, $\rho = \rho_0 + m_w$, ρ_0 [kg.m^{-3}] being the initial total homogenized specific mass and m_w [kg.m^{-3}] the mass content of water, that is the mass of water dm_w that entered or left an elementary volume dV of the porous medium since the initial state, divided by dV. The vector $\boldsymbol{M}_w$ [kg.m^{-2}.s^{-1}] appearing in Eq. (2) is the mass flow of water. Concerning Eq. (3), h_w^m [J.kg^{-1}] is the specific enthalpy of water, Q [J.m^{-3}] is the "non-convective" heat and q [J.m^{-2}.s^{-1}] the heat flow due to conduction. The radioactivity of rocks is taken into account through the heat source term θ [W.m^{-3}]. The balance equations must be supplemented with constitutive equations. Firstly, we use the classical decomposition of the Cauchy stress tensor into two contributions: $\boldsymbol{\sigma} = \boldsymbol{\sigma}' + \sigma_p \boldsymbol{I}$ with $\boldsymbol{\sigma}'$, the effective Cauchy stress tensor for the solid grains behaviour and σ_p, the hydraulic stress. In this work, the behavior of solid grains is assumed to be thermo-elastic and linear, so that we can introduce the linear total strain $\boldsymbol{\epsilon}$ and the drained elasticity tensor **C** with the following incremental law: $d\boldsymbol{\sigma}' = \mathbf{C}:(d\boldsymbol{\epsilon} - \alpha_0 dT\, \mathbf{I})$, in which α_0 stands for the thermal dilation of the dry material, T the absolute temperature and **I** the unit tensor. Below, we denote by E and ν the drained Young's modulus and Poisson's ratio respectively. The porous behavior is described by the incremental evolution of the Eulerian porosity ϕ and the hydraulic stress σ_p (Coussy, 2004):

$$d\phi = (b - \phi)\left(d\epsilon_v - 3\alpha_0\, dT + \frac{dp_w}{K_s}\right) \tag{4}$$

$$d\sigma_p = -b\, dp_w \tag{5}$$

where b is the Biot coefficient, $\epsilon_v = \boldsymbol{Tr}(\boldsymbol{\epsilon})$ is the volume total strain, p_w the water pressure and K_s the bulk modulus of solid grains. The mass content of water can then be expressed as the variation of water mass per unit of volume between the actual state and the initial state: $m_w = \rho_w(1+\epsilon_v)\phi - \rho_w^0 \phi_0$, with ρ_w^0 the initial specific mass of water and ϕ_0 the initial porosity. The hydraulic and thermal phenomena are governed by the Darcy's law and Fourier's law respectively, and most rock properties (like the specific heat at constant stress c_0^σ or the thermal conductivity λ) are assumed to depend on temperature T and/or porosity ϕ. More precisely, if we denote by K_{int} the intrinsic permeability, we consider the following relations:

$$\boldsymbol{q} = -\lambda \nabla T \quad \text{and} \quad \boldsymbol{M}_w = \frac{\rho_w K_{int}}{\mu_w}(-\nabla \mathrm{p_w} + \rho_w \boldsymbol{F}^m) \qquad (6) \text{ and } (7)$$

In Eq. (3), the non-convected heat Q can be understood as the "variation of heat per unit of volume not coming from convection nor conduction". It comes from the heat produced by the volume deformation of solid grains and water but also from the internal energy of the homogenized medium.

In an attempt to characterize as precisely as possible the convective movement of water and the associated heat flow, the properties of water (specific mass $\rho_w(T, p_w)$, specific enthalpy $h_m^w(T, p_w)$, dynamic viscosity $\mu_w(T)$, and specific heat $c_w^p(T)$) are assumed to depend on the pressure and/or temperature. We used the properties either of pure water or brine (Zaytsev and Aseyev, 1992, Haynes, 2012). The considered rheology of the circulating fluid is thus governed by the two following equations:

$$\frac{d\rho_w}{\rho_w} = \frac{dp_w}{K_w} - 3\alpha_w\, dT \quad \text{and} \quad dh_w^m = c_w^p(T)dT + (1 - 3\alpha_w \mathrm{T})\frac{dp_w}{\rho_w} \qquad (8) \text{ and } (9)$$

with K_w the (constant) bulk modulus of water. Eq. (8) was already used in the work of Segall and Rice (2006). For the dynamic viscosity $\mu_w(T)$, we used an exponential law with the temperature, for the thermal conductivity $\lambda_w(T)$ and the specific heat $c_w^p(T)$, we used quadratic laws (Haines 2012).

3. NUMERICAL MODEL

The geological layers considered in this work are slightly adapted from the idealized cross section presented in the paper of Guillou-Frottier et al. (2013) and inspired by the contribution of Genter et al. (1997); Genter and Traineau (1992). We only consider 6 layers: the three first layers correspond to the sedimentary cover, i.e. Tertiary to Jurassic marls and clays between 0 and 800m of depth, Keuper and Muschelkalk formations between 800m and 1000 m, and Buntsandstein sandstones between 1000 m and 1400 m. The granitic basement is represented by three other layers corresponding to the different petrographic units of the granite massif. On top, a thin layer between 1400m and 1550m is considered to reproduce the strongly altered granite from the paleo-erosion surface. The second layer, between 1550m and 3700 m, corresponds to a more fractured monzonitic granite in which the homogenized permeability is high. The last layer, located between 3700m and 5350 m, corresponds to a crystalline unit made of a porphyritic monzogranite and a fine grained two mica-granite. The height of the model corresponds to the height of the measured temperature profile obtained in GPK2, see e.g. Pribnow and Schellschmidt (2000). The six layers are meshed with QUAD elements (see figure 1) performing an eight-term polynomial interpolation of mechanical displacements and a four-term polynomial interpolation of pressures and temperatures. Below, we denote by x the horizontal direction inside the mesh, y the vertical direction, and z the out of plane direction perpendicular to it.

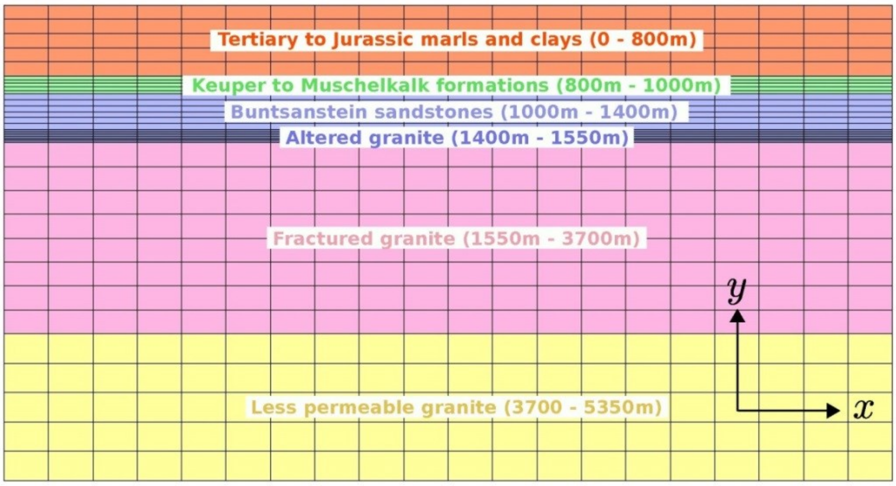

Figure 1: Idealized cross section of the Soultz-sous-Forêts reservoir (10kmx5.5km) meshed with 20x50 QUAD elements in 6 geological layers: 3 for the sedimentary cover (Tertiary and Jurassic, Upper and middle Trias, and lower Trias) and 3 for the Paleozoic granitic basement (paleo-altered granite, fractured porphyritic monzogranite and the lower intrusive two-mica granite).

The boundary conditions of the problem are the following: normal mechanical displacement is nul and no friction is considered on the lateral and lower boundaries of the domain, while the upper boundary is stress free. For thermal aspects, a temperature of 15°C and 208°C is imposed on the upper and lower boundary respectively. These values are directly taken from the experimental temperature profile shown in figure 6. The thermal flow vanishes on lateral facets. For hydraulic aspects, the flow vanishes on all boundaries except the upper one for which the water pressure equals the atmospheric pressure, i.e. p_w = 0.1MPa. Figure 2 summarizes the entire set of boundary conditions.

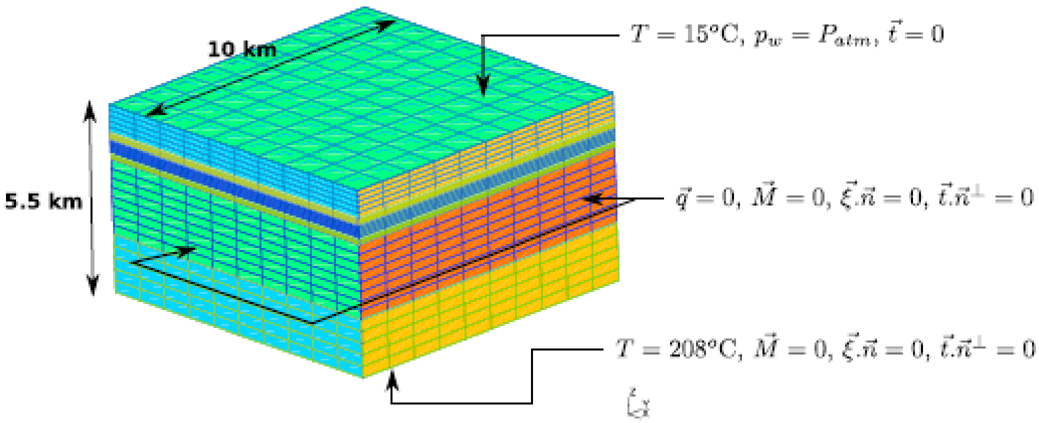

Figure 2: boundary conditions: imposed displacement on the sides and below, free boundary condition on the top, imposed temperature below (208°C) and above (15°C), no flux on the sides.

The simulation is carried out with the assumption of plane strains (in the x, y plane) by using the French finite element software Code Aster. Some routines of the latter have been overloaded to integrate the constitutive equations presented above. At first, the boundary conditions and gravity are progressively applied during a "short" period of 1000 years. In a second step, the code iterates with a time increment equal to 10000 years until a stationary state is reached. A stationary state is here defined by using three convergence indicators $I_n(\boldsymbol{X})$ involving the generalized displacements $\boldsymbol{X} \equiv (\xi, p_w, T)$ calculated for different time increments t_n. More precisely, a stationary state is reached if: $I_n(\boldsymbol{X}) = \frac{\max(X_{\{n+1\}} - X_n)}{\Delta X^*} < 1$ with: $\Delta\xi^* = 1m$, $\Delta p_w{}^* = 0.05MPa$, and $\Delta T^* = 0.1K$ for 15 consecutive time increments t_n.

4. RESULTS AND DISCUSSION

The permeability profile is a key parameter for the hydro-thermal circulation (see Table 1). The value in the fractured granite between 1550 m and 3700 m is set to $k = 3.0\ 10^{-15}\ m^2\ (i.e.\ 3\ mD)$.

Table 1: permeability profile in the geothermal reservoir at Soultz-sous-Forêts

	Geological layers	Depth (m)	Permeability (mD)
1	Tertiary and Jurassic formations	0-800	0.001
2	Muschelkalk formations	800-1000	0.01
3	Buntsandstein sandstones	1000-1400	0.5
4	Altered granite	1400-1550	5
5	Fractured porphyritic monzogranite	1550-3700	3
6	Fine-grained two-mica granite	3700-5350	0.001

The temperature map of the obtained stationary state (see Figure 3) clearly shows convection loops having a size of about 1.3 km. Two other simulations with a model of 20km and 30km in width proved that the cell width is quasi constant independently of the model width.

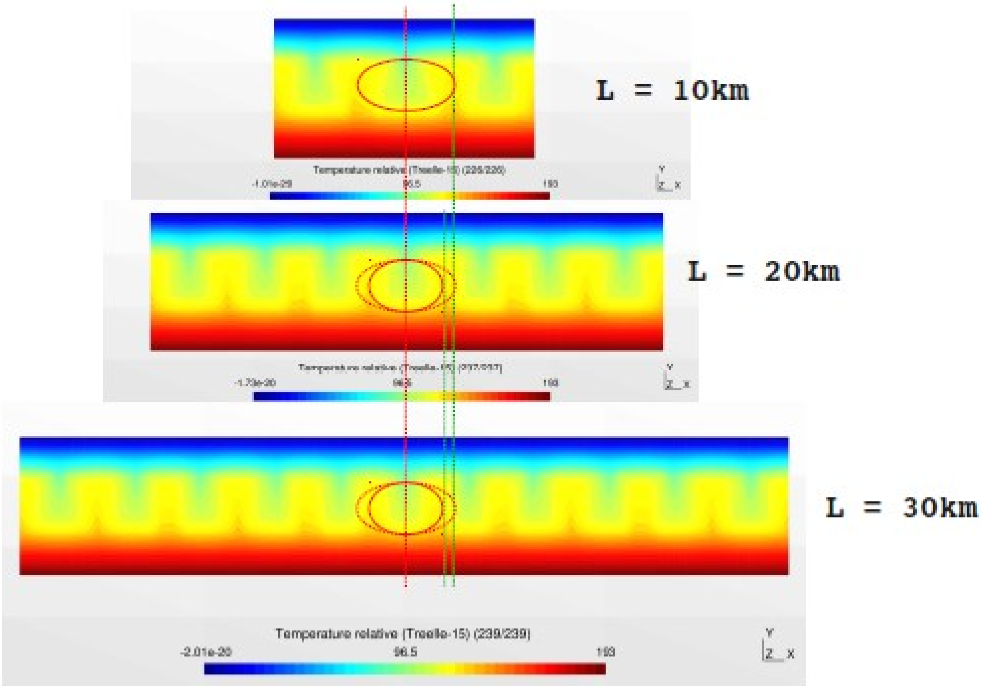

Figure 3: Temperature maps for three different width of the model: L=10, 20 and 30 km. The color coded temperature has a similar pattern independently of the system width. The size of the periodic pattern is of the order of 3 km and corresponds to a pair of convective cells.

Figure 4 shows the influence of the permeability of layer 5 (fractured granite) on the onset of convection. It shows that the effective permeability at large scale of the fractured granite is at the critical value for developing hydro-thermal loops. Vertical profiles of the water pressure keeps globally hydrostatic. The order of magnitude of the vertical Darcy velocity $V_y = M_w \cdot e_y / \rho_w$ in the fractured granite is 30 cm.year^{-1}, which is in accordance with the value 15 cm.year^{-1} obtained by Guillou-Frottier et al. (2013) using slightly different permeability profiles.

We performed a sensitivity analysis of the different parameters that enter the numerical modeling on the convective solution. We show that the thermal conductivity of the fluid $\lambda_w(T)$, the heat radioactive source magnitude θ, the specific heat of the fluid $c_w^p(T)$, the dynamic fluid viscosity $\mu_w(T)$ and the fluid permeability K_{int}. These sensitivities show once again that the rheology of waters seems to have a great impact on the vertical profile of temperature.

5. CONCLUSIONS

The two dimensional numerical model developed in this work lead us to the following main conclusions. The order of magnitude of the convective cell size in the reservoir is about 1.5 km, a value being independent of the model width. A periodic pair of cells is then 3 km wide. There is no sensible variation of porosity in the reservoir. It would be possible to make the assumption $d\phi = 0$ in future works to simplify the constitutive equations. The order of magnitude of the maximal vertical Darcy velocity is 30 cm.year^{-1}, a value confirmed by previous works found in the literature. The field of water pressure keeps globally hydrostatic, and the influence of thermo-hydraulic coupling on the vertical stress state of the reservoir is low. The rheology of water seems to play a crucial role on the vertical profile of temperature. An experimental investigation to measure the properties of the natural geothermal brine would be of great interest to refine the results presented here. These conclusions have been obtained with a two dimensional model under the assumption of plane strains. They should consequently be confirmed or infirmed by a three dimensional model. The effect of local main faults in the reservoir on the global circulation is also part of an on-going study. Stress perturbations related to significant temperature fluctuations in the reservoir are presently studied as their implications on location of induced seismicity.

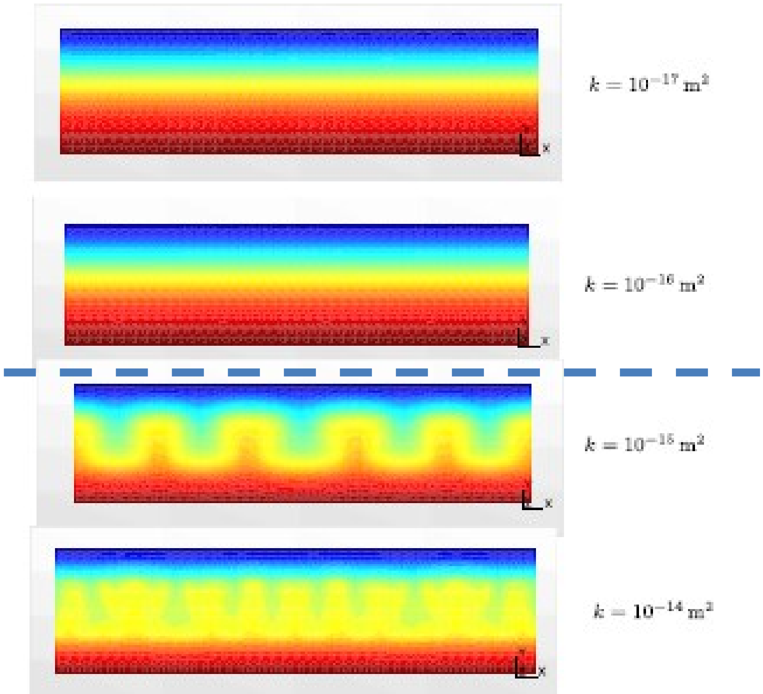

Figure 4: Temperature map for different permeability of the fractured granite layer: from k=10^{-17} m^2 (top) to k=10^{-14} m^2 (below). The critical value for the onset of a large scale convection is at k~10^{-15} m^2.

ACKNOWLEDGMENTS

The authors gratefully acknowledge Dr. François Cornet for the helpful discussions. This work has been published under the framework of the LABEX ANR-11-LABX-0050-G-EAU-THERMIE-PROFONDE and benefits from a funding from the state managed by the French National Research Agency as part of the "Investments for the Future" program.

REFERENCES

Bächler D., and T. Kohl. Coupled thermal-hydraulic-chemical modelling of enhanced geothermal systems. Geophysical Journal International, 161:533–548, 2005.

Bächler, D. T. Kohl, and L. Rybach. Impact of graben-parallel faults on hydrothermal convection — Rhine Graben case study. Physics and Chemistry of the Earth, 28:431–441, 2003.

Cerminara M. and A. Fasano. Modeling the dynamics of a geothermal reservoir fed by gravity driven flow through overstanding saturated rocks. Journal of Volcanology and Geothermal Research, 233-234:37–54, 2012.

Coussy, O., Poromechanics. John Wiley & Sons, 2004.

Gelet, R., B. Loret, and N. Khalili. A thermo-hydro-mechanical coupled model in local thermal non-equilibrium for fractured HDR reservoir with double porosity. Journal of Geophysical Research, 117:1–23, 2012.

Genter, A., C. Castaing, C. Dezayes, H. Tenzer, H. Traineau, and T. Villemin. Comparative analysis of direct (core) and indirect (borehole imaging tools) collection of fracture data in the Hot Dry Rock Soultz reservoir (France). Journal of Geophysical Research, 102:15419–15431, 1997.

Genter, A. and H. Traineau. Borehole EPS1, Alsace, France: preliminary geological results from granite core analyses for Hot Dry Rock research. Scientific Drilling, 3:205–214, 1992.

Guillou-Frottier, L., C. Carré, B. Bourgine, V. Bouchot, and A. Genter. Structure of hydrothermal convection in the Upper Rhine Graben as inferred from corrected temperature data and basin-scale numerical models. Journal of Volcanology and Geothermal Research, 256:29–49, 2013.

Haynes, W. M., Handbook of Chemistry and Physics. CRC Press, 93 edition, 2012.

Kohl, T., K. F. Evans, R. J. Hopkirk, and L. Rybach. Coupled hydraulic, thermal and mechanical considerations for the simulation of hot dry rock reservoirs. Geothermics, (3):345–359, 1995.

Kohl, T., D. Bächler, and L. Rybach. Steps towards a comprehensive thermo-hydraulic analysis of the HDR test site Soultz-sous-Forêts. Proceedings World Geothermal Congress, 2000.

Kohl T. and T. Mégel. Predictive modeling of reservoir response to hydraulic stimulations at the European EGS site Soultz-sous-Forêts. International Journal of Rock Mechanics and Mining Science, (44):1118–1131, 2007.

Pasquale, V., M. Verdoya, and P. Chiozzi. Groundwater flow analysis using different geothermal constraints: The case study of Acqui Terme area, northwestern Italy. Journal of Volcanology and Geothermal Research, (199): 38–46, 2011.

Pribnow D. and R. Schellschmidt. Thermal tracking of upper crustal fluid flow in the Rhine graben. Geophysical Research Letters, (13):1957–1960, 2000.

Segall, P. and J. R. Rice. Does shear heating of pore fluid contribute to earthquake nucleation? Journal of Geophysical Research, (111):1–17, 2006.

Zaytsev I.D. and G.G. Aseyev, Properties of Aqueous Solutions of Electrolytes, CRC Press Inc, 1992.